Cell, Vol. 121, 579–591, May 20, 2005, Copyright ©2005 by Elsevier Inc. DOI 10.1016/j.cell.2005.03.016

Specific Ablation of the Apoptotic Functions of Cytochrome c Reveals a Differential Requirement for Cytochrome c and Apaf-1 in Apoptosis

Zhenyue Hao,[1,2,3,*] Gordon S. Duncan,[1,2,3] Chia-Che Chang,[1,2,3,5] Andrew Elia,[1,2,3] Min Fang,[4] Andrew Wakeham,[1,2,3] Hitoshi Okada,[1,2,3] Thomas Calzascia,[1,2,3] YingJu Jang,[1,2,3] Annick You-Ten,[1,2,3] Wen-Chen Yeh,[1,2,3] Pamela Ohashi,[1,2,3] Xiaodong Wang,[4] and Tak W. Mak[1,2,3,*]

[1]The Campbell Family Institute for Breast Cancer Research

[2]Ontario Cancer Institute
University Health Network

[3]Departments of Immunology and Medical Biophysics
University of Toronto
Toronto, Ontario M5G 2C1
Canada

[4]Howard Hughes Medical Institute and Department of Biochemistry
University of Texas Southwestern Medical Center at Dallas
Dallas, Texas 75390

Summary

As components of the apoptosome, a caspase-activating complex, cytochrome c (Cyt c) and Apaf-1 are thought to play critical roles during apoptosis. Due to the obligate function of Cyt c in electron transport, its requirement for apoptosis in animals has been difficult to establish. We generated "knockin" mice expressing a mutant Cyt c (KA allele), which retains normal electron transfer function but fails to activate Apaf-1. Most KA/KA mice displayed embryonic or perinatal lethality caused by defects in the central nervous system, and surviving mice exhibited impaired lymphocyte homeostasis. Although fibroblasts from the KA/KA mice were resistant to apoptosis, their thymocytes were markedly more sensitive to death stimuli than *Apaf-1*$^{-/-}$ thymocytes. Upon treatment with γ irradiation, procaspases were efficiently activated in apoptotic KA/KA thymocytes, but Apaf-1 oligomerization was not observed. These studies indicate the existence of a Cyt c- and apoptosome-independent but Apaf-1-dependent mechanism(s) for caspase activation.

Introduction

The mitochondrion is a key element of intrinsic apoptosis induced by cellular stress (Green and Reed, 1998; Wang, 2001). Upon initiation of this cascade, proapoptotic Bcl-2 family members trigger oligomerization and activation of the death effectors Bax and Bak, which permeabilize the outer mitochondrial membrane (Kluck et al., 1999). Cytochrome c (Cyt c) is then released from the intermembrane space of the mitochondrion into the cytosol, where it binds to apoptotic protease-activating factor 1 (Apaf-1) in the presence of ATP/dATP to form the apoptosome (Li et al., 1997). This multimeric Apaf-1/Cyt c complex recruits procaspase-9 via its caspase recruitment domain (CARD), promoting procaspase-9's efficient activation (Rodriguez and Lazebnik, 1999; Zou et al., 1999). Activated caspase-9 in turn activates the downstream effectors caspase-3 and -7 (Liu et al., 1996; Li et al., 1997), which rapidly cleave intracellular substrates. Morphological changes characteristic of apoptosis result, such as cell shrinkage, plasma membrane blebbing, chromatin condensation, and the formation of apoptotic bodies (Hengartner, 2000).

Apoptosis is essential to the construction, maintenance, and repair of mammalian tissues, particularly the immune and central nervous systems (CNS) (Meier et al., 2000; Rathmell and Thompson, 2002; Yuan and Yankner, 2000). In the immune system, T and B lymphocytes are constantly generated from the thymus and bone marrow (BM), respectively. Lymphocytes with nonfunctional or self-reactive antigen receptors die via apoptosis (Rathmell and Thompson, 2002) such that only 1%–2% of these cells complete maturation. Antigen-activated peripheral T and B cells proliferate exponentially, but lymphocyte homeostasis is maintained by the apoptotic death of these cells upon antigen clearance. Antiapoptotic Bcl-2 family members are critically involved in lymphocyte homeostasis. Transgenic expression of *Bcl-2* or *Bcl-x*$_L$ results in lymphocyte accumulation (Chao et al., 1995; Grillot et al., 1995), while ablation of *Bcl-2* (Veis et al., 1993) or *Bcl-x*$_L$ (Ma et al., 1995; Motoyama et al., 1995) leads to a loss of mature or developing lymphocytes, respectively. Similar findings were reported for conditional ablation of *MCL-1* (Opferman et al., 2003). Disruption of *Bim* (Bouillet et al., 1999; Bouillet et al., 2002) or combined *Bax/Bak* deficiency (Lindsten et al., 2000; Rathmell et al., 2002) causes splenomegaly, lymphadenopathy, and defects in thymic negative selection. In the embryonic CNS, normal development depends on a wave of immature neuron death mediated by mitochondrion-mediated apoptosis (Yuan and Yankner, 2000). In mice, disruption of this wave via inactivation of *Apaf-1*, *caspase-9*, or *caspase-3* results in embryonic or postnatal lethality (Cecconi et al., 1998; Hakem et al., 1998; Kuida et al., 1998; Kuida et al., 1996; Woo et al., 1998; Yoshida et al., 1998). *Cyt c* null mutants survive until E8.5 with reduced size and delayed development (Li et al., 2000). However, given that Cyt c's primary role in the cell is electron transport, these phenotypes likely result from defective oxidative phosphorylation rather than impaired apoptosis.

The early embryonic lethality associated with null mutation of *Cyt c* precludes analysis of the role of Cyt c-mediated apoptosis in development and tissue homeostasis. We therefore used gene targeting to disrupt

*Correspondence: zyhao@uhnres.utoronto.ca; tmak@uhnres.utoronto.ca

[5]Present address: Institute of Biomedical Sciences, National Chung Hsing University, 250 Kuo Kuang Road, Taichung 402, Taiwan.

the proapoptotic function of Cyt c while preserving its electron-transport function. Lysine 72 of the Cyt c protein appears critical only for its apoptotic function. Yeast Cyt c has normal respiratory function but lacks apoptotic function due to lysine 72 trimethylation (Kluck et al., 2000). In mammalian cells, mutation of lysine 72 to alanine (K72A) abolishes Cyt c binding to Apaf-1 and reduces caspase-3 activity by 10-fold (Yu et al., 2001). We report here on *Cyt c* "knockin" mice in which a K72A mutation specifically abolishes the apoptotic function of Cyt c. We demonstrate that loss of Cyt c-mediated apoptosis disturbs brain development and has intrinsic and extrinsic effects on lymphocyte homeostasis.

Results

Generation of KA/KA Knockin Mice

The K72A (KA) knockin allele was introduced into the murine genomic *Cyt c* locus in embryonic stem (ES) cells by homologous recombination (Figure S1A). Southern blotting confirmed the integration of the KA allele in 3 of 300 G418-resistant clones, with no random integration of *neo*^{r} (Figure S1B). Sequencing of the targeted *Cyt c* allele in all three homologous recombinants confirmed the correct introduction of the mutation (data not shown). Three independent lines of homozygous KA/KA mice were generated that showed no phenotypic differences. Genotypes were confirmed by PCR using primers able to distinguish the wild-type (wt) *Cyt c* allele from the KA allele after deletion of the *loxP*-flanked cassette (Figure S1C).

Perinatal Lethality of KA/KA Mice

KA/KA mice were born at a frequency of 12%, much lower than the expected Mendelian ratio (Table S1). Of these, 16 of 37 had forehead protrusions and died within 1–2 days. Timed gestational dissections revealed that KA/KA embryos were present at E14.5 at the expected Mendelian frequency. About 25% of E14.5 mutant embryos showed abnormal brain morphology in the form of ectopic masses with exencephalic defects and were clearly not destined to develop a skull or survive to birth. Compared to control mice (Figures 1A, 1B, and 1G), KA/KA mice showed expansions of the cortex and midbrain (Figures 1C–1E and 1H) that caused cranial enlargement. Overgrowth of cortical neural tissue and ventricular-zone expansion were evident in histological sections of mutant brains (Figures 1E and 1H). The rostral expansion of the forebrain ("cauliflowerlike mass") described in *Apaf-1*$^{-/-}$ mice was also observed in KA/KA mice (Figure 1F). When the distribution of proliferating cells was examined in histological sections of wt (Figures 1I and 1L) or KA/KA (Figures 1J and 1M) brains using BrdU incorporation, ectopic clusters of proliferating cells were observed in mutant brains that corresponded to the forehead protrusions (Figure 1K).

The exencephalic phenotype of postnatal day 1 (P1) KA/KA animals (Figure 1N) recapitulated that of *Apaf-1*$^{-/-}$ and *caspase-9*$^{-/-}$ mice. Ventricular-zone expansion and neural tissue overgrowth were evident in histological sections. Comparison of the dissected brains of P1 control (Figure 1O) and KA/KA (Figure 1P) mice revealed neocortical deterioration, intracerebral hemorrhage, and midbrain expansion.

Normal Cyt c Release and Respiratory Function but Impaired Caspase Activation in KA/KA MEFs

We next determined the effect of the KA mutation on Cyt c functions. Base levels of Apaf-1 and caspase-9 proteins were comparable in murine embryonic fibroblasts (MEFs) prepared from KA/KA and KA/+ E14.5 embryos (Figure 2A). KA/KA and KA/+ MEFs subjected to UV irradiation and immunostaining showed no differences in Cyt c release into the cytoplasm or in the proportion of Cyt c-releasing cells (Figure 2B). A relative decrease in cytoplasmic volume was observed in UV-treated KA/+ MEFs; this decrease was likely due to apoptosis-mediated shrinkage. When oxygen consumption was measured as an index for respiration rate, no differences were found (Figure 2C and Table S2). The mutated Cyt c protein is thus released normally upon apoptotic stimulation and has intact respiratory function. However, biochemical analysis in a cell-free system showed that neither procaspase-3 nor procaspase-9 could be cleaved in KA/KA MEF extracts (Figure 2D). The procaspase-3 cleavage defect was rescued when recombinant Cyt c was added (Figure 2E). Thus, the lysine-to-alanine substitution at residue 72 in Cyt c severely impairs its ability to activate caspases.

Resistance of KA/KA MEFs to UV and Staurosporine in the Absence of Apoptosome Formation

We examined the sensitivity of KA/+, KA/KA, and *Apaf-1*$^{-/-}$ MEFs to various apoptotic stimuli. MEFs of all genotypes were viable at 6 hr post-UV irradiation (120 mJ/cm^2) (Figure 3A, left). However, while the viability of KA/+ MEFs had declined drastically by 24 hr post-UV, the majority of KA/KA and *Apaf-1*$^{-/-}$ MEFs survived. By 36 hr post-UV, only 7.5% of KA/+ MEFs were viable, whereas 64% of KA/KA and 81% of *Apaf-1*$^{-/-}$ MEFs survived. The majority of KA/+ MEFs also showed decreased mitochondrial membrane potential at 24 hr and 36 hr post-UV, whereas the majority of KA/KA and *Apaf-1*$^{-/-}$ cells retained normal membrane potential (Figure 3A, right). KA/KA MEFs were also resistant to staurosporine (Figure 3B). Consistent with the viability analysis, nuclear condensation was extensive in UV-irradiated KA/+ MEFs but undetectable in KA/KA and *Apaf-1*$^{-/-}$ MEFs (Figure 3C). Caspase-3 activity was impaired in UV-treated KA/KA MEFs (Figure 3D), and Apaf-1 oligomerization did not occur (Figure 3E). Thus, the KA mutation efficiently abolishes Cyt c binding to Apaf-1 and blocks apoptosome formation required for procaspase activation, rendering the MEFs resistant to apoptotic stimuli.

Cachexia, Hydrocephalus, and Lymphopenia in Juvenile KA/KA Mice

More than half of surviving KA/KA mice developed severe cachexia such that they achieved only about 50% of normal body weight by age 3–4 weeks (Table S1; Figure 4A). Spinning (running in circles with a bias toward one direction or the other), weakness, occasional hindleg paralysis, and an uncoordinated walk appeared with increasing age, culminating in death at age 3–4

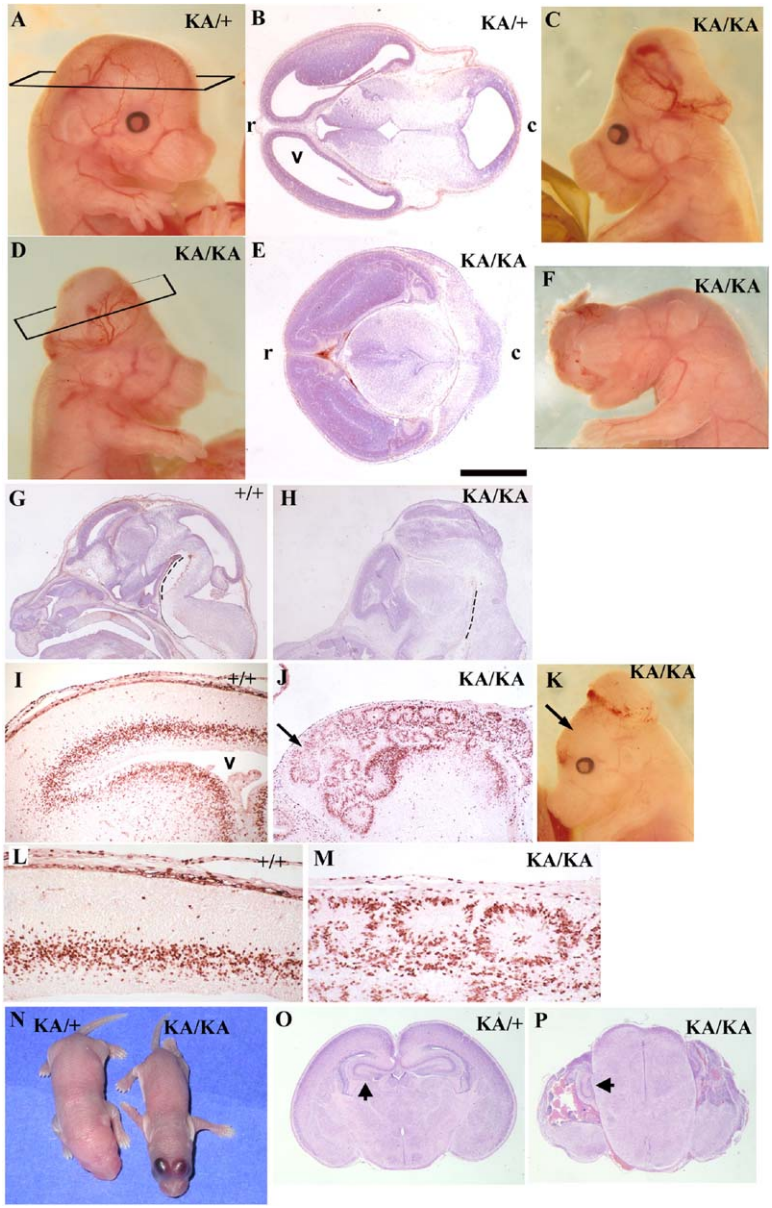

Figure 1. Gross and Histological Analyses of the Neural Phenotype of KA/KA Mice

Whole mounts of KA/+ control E14.5 embryos (A) and KA/KA mutant E14.5 embryos (D) showing the planes of horizontal section through the brains are histologically presented in (B) (KA/+) and (E) (KA/KA). Ventricles (v) in the control embryo (B) are clearly seen as open spaces, whereas overexpansion of both the cortex and midbrain in the mutant (E) obliterates most of the ventricular spaces. (C) and (F) show other examples of cortical overgrowth in KA/KA embryos. Normal flexures and development of the midbrain/hindbrain in a control E14.5 embryo (G) are distorted by overgrowth in the mutant (H). Dotted lines in (G) and (H) indicate the separation of midbrain and hindbrain. (I) and (J) show midsagittal sections of a BrdU-labeled KA/+ E14.5 embryo (I) showing normal proliferating cells in a narrow band next to the ventricle and a KA/KA E14.5 embryo (J) showing ectopic sites of proliferation in the cortex. (L) and (M) show higher magnifications of (I) and (J), respectively. (K) shows a whole mount of the mutant embryo sectioned in (J). Arrows in (J) and (K) indicate corresponding points. (N) shows a dorsal view of brain protrusion in a P1 KA/KA pup. (O) and (P) show midcoronal plane of section through P1 control (O) and KA/KA (P) brains (arrows, hippocampal formation). The enlarged midbrain has forced the hippocampus laterally in the mutant (P), and the dorso-lateral cortex is damaged with evidence of hemorrhage. Other abbreviations: c, caudal; r, rostral. Magnifications of embryos in (A), (C), (D), (F), and (K) are comparable. Scale bar: (B) and (E) = 850 μm; (G), (H), (O), and (P) = 1.3 mm; (I) = 300 μm; (J) = 600 μm; (L) and (M) = 150 μm.

weeks. Those viable mutant mice without cachexia displayed the spin phenotype, particularly when stressed. Hydrocephalus was prominent in 3- to 4-week-old moribund KA/KA mice. Dissection of the brains of these animals revealed severe damage to the neocortex, with most of the cellular contents replaced by cerebrospinal fluid (CSF) (Figure 4B and data not shown). Histological analysis showed that most of the cortical structure had been lost and that the thalamus and hypothalamus were reduced in size (Figure 4C).

Surprisingly, flow cytometric analysis of the lymphoid tissues of moribund KA/KA mice showed an absence of $CD4^+CD8^+$ cells in the thymus. Total thymic cellularity was reduced by 100-fold compared to littermate controls (Figure 4D). Pre-B cells were not detected in the BM, and splenic T and B cell numbers were decreased by 50-fold. However, there were no significant differences between mutants and controls in myeloid cell numbers in spleen or BM (data not shown). At birth, T cell development in the mutant thymus appeared normal (data not shown). At age 2 weeks, T cell development in the thymus, B cell development in the BM, and lymphocyte cellularity in the spleen and lymph nodes were relatively normal in wasting (but not moribund) KA/KA mice after correction for their smaller size (data not shown). To investigate whether the lymphocyte defects observed in moribund KA/KA mice were intrinsic to these cells or due to external factors, we transferred BM cells of mutant mice that had developed severe lymphopenia into *Rag-1* (recombination activating gene 1) deficient recipients that had been sublethally irradiated (600 rads). T cell development in the thymus, B cell development in the BM, and the cellularity of T and B cells in the peripheral lymphoid organs of the recon-

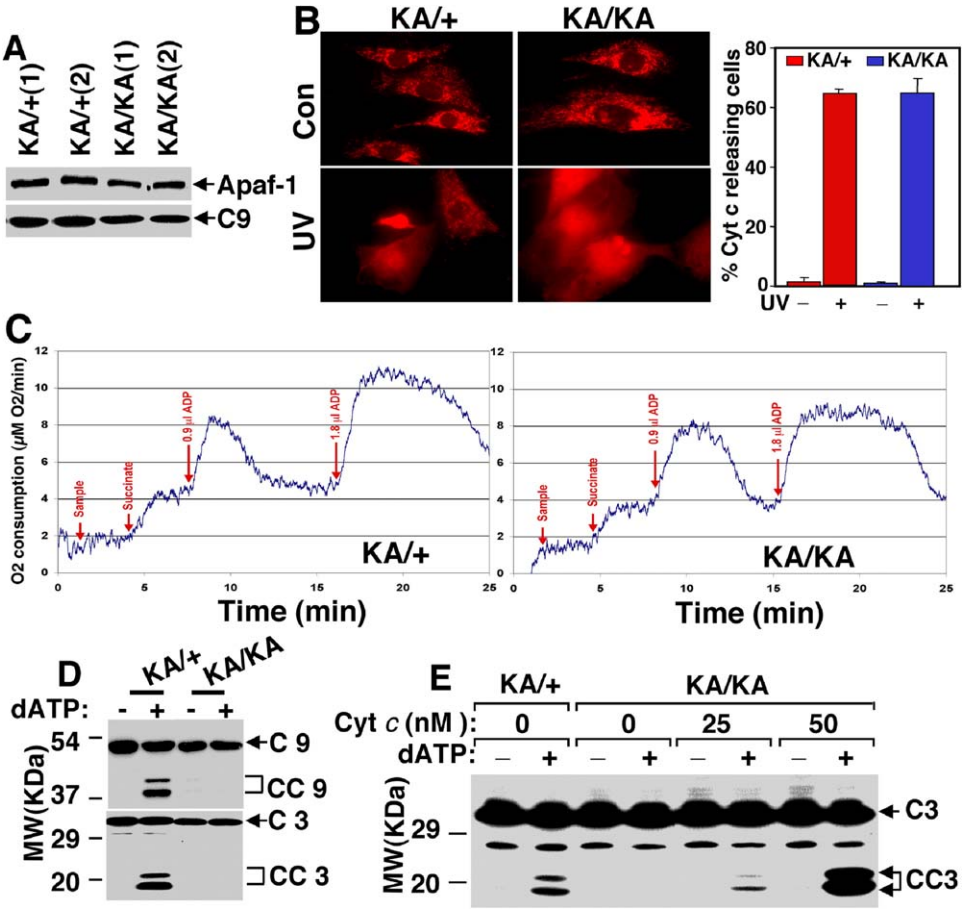

Figure 2. Intact Respiratory Function but Impaired Caspase Activation in KA/KA MEFs

(A) Western blot of basal levels of Apaf-1 and caspase-9 proteins in MEFs from KA/+ and KA/KA mice.

(B) Immunostaining showing normal Cyt c release from mutant mitochondria into the cytosol in response to UV (10 mJ/cm^2) (left panel). The proportion of cells releasing Cyt c in response to UV was equivalent in KA/+ and KA/KA MEFs (right panel). Error bars represent standard deviations from the mean of three experiments.

(C) Respiratory-function analysis showing normal oxygen consumption in KA/KA MEFs upon addition of succinate and ADP.

(D) Western blot showing impaired dATP-dependent procaspase-3 (C3) and procaspase-9 (C9) cleavage in extracts of KA/KA MEFs in vitro. CC3, cleaved caspase-3; CC9, cleaved caspase-9.

(E) Western blot showing the full restoration of impaired dATP-dependent procaspase-3 cleavage in extracts of KA/KA MEFs upon addition of recombinant Cyt c in vitro.

stituted mice were comparable to those in recipients reconstituted with BM cells from controls (Figure 4E). Thus, the development of thymic atrophy and loss of peripheral lymphocytes in juvenile KA/KA mice is an extrinsic defect.

Association of Impaired Growth-Hormone Production with Lymphopenia and Cachexia in KA/KA Mice

To identify the external factors underlying the lymphocyte defects in KA/KA mice, we examined marker expression in the hypothalamus. Disruption of hypothalamic function can cause wasting and early postnatal lethality (Nakai et al., 1995; Schonemann et al., 1995). However, the expression of vasopressin, neuropeptide Y, and growth-hormone-releasing hormone (GHRH) were all comparable in KA/KA mice and littermate controls (data not shown). Thymocytes are known to be exquisitely sensitive to glucocorticoid-induced apoptosis (Wyllie, 1980). However, serum glucocorticoid levels in lymphopenic KA/KA mice were normal (data not shown). Moribund KA/KA mice also showed normal serum TNFα levels and blood cultures negative for bacteria (data not shown), ruling out septicemia. Serum glucose levels were also normal. Gross histological analysis of moribund mice showed no obvious pathological changes in lungs, heart, kidneys, liver, pancreas, or stomach except the previously noted severe damage to the cortex and opportunistic infections in the intestinal tract (Figures 4B and 4C and data not shown).

To determine if the brain damage in KA/KA mice affected their endocrine-gland function, we examined the adrenal, thyroid, and pituitary glands of these animals. H&E staining revealed normal adrenal and thyroid glands (data not shown). However, the pituitary gland in mutant neonates was thinner and longer than in con-

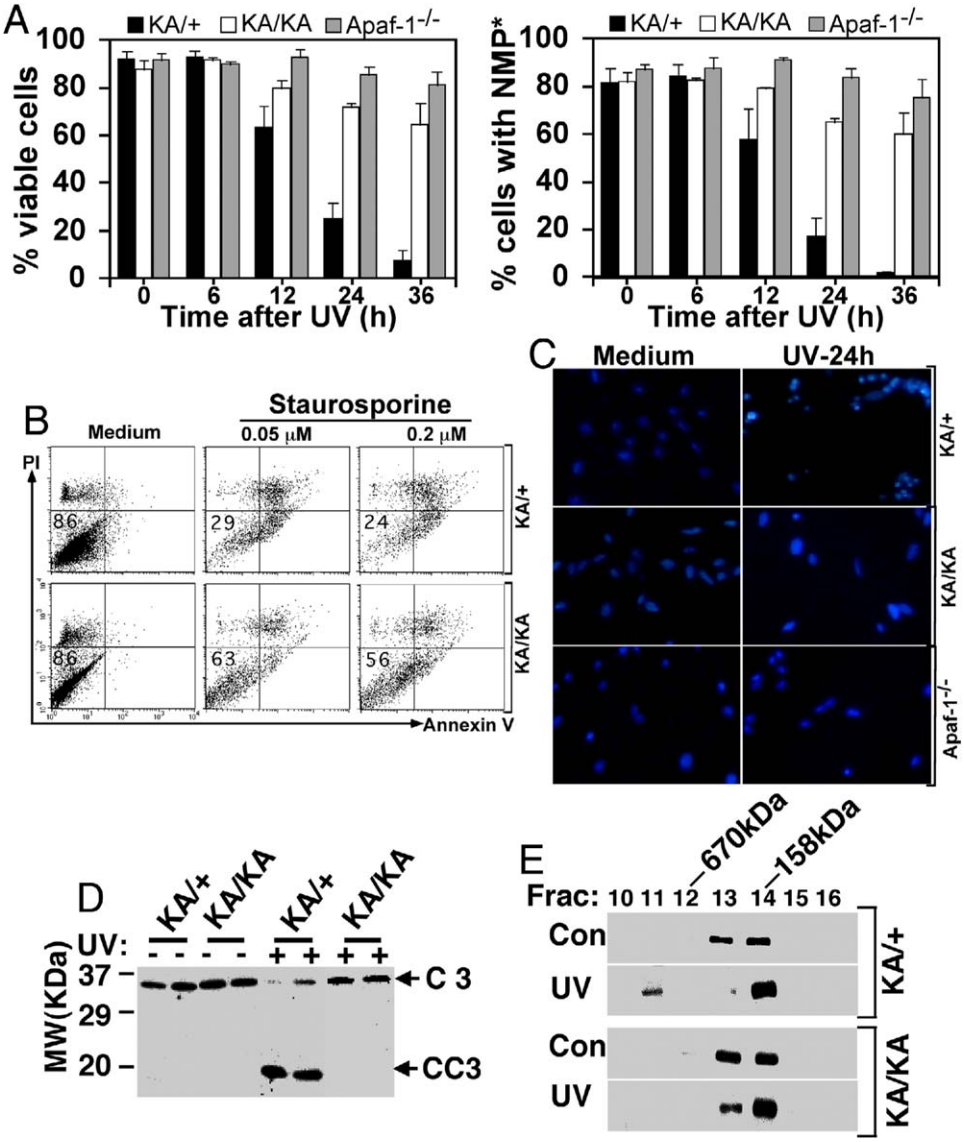

Figure 3. Resistance of KA/KA MEFs to UV Irradiation and Staurosporine

(A) Mean percentages ±SD of viable cells (left panel) and cells with normal mitochondrial transmembrane potential (right panel) retained in KA/+, KA/KA, and *Apaf-1*$^{-/-}$ MEFs (n = 3–5) at the indicated time points after UV irradiation (120 mJ/cm^2). NMP*, normal mitochondrial transmembrane potential.

(B) Flow cytometric analyses of the percent viability of KA/+ and KA/KA MEFs 24 hr after treatment with staurosporine and staining with PI and annexin V.

(C) Lack of chromatin condensation in KA/KA and *Apaf-1*$^{-/-}$ MEFs at 24 hr post-UV (120 mJ/cm^2).

(D) Western blot showing impaired procaspase-3 cleavage in mutant MEFs subjected to UV (10 mJ/cm^2).

(E) Defective Apaf-1 oligomerization. Extracts of UV-irradiated (10 mJ/cm^2) MEFs were fractionated (10–16) according to molecular weight. Apaf-1 monomers and oligomers were located in fractions 13/14 and 10/11, respectively.

trols (Figure 5A). Immunohistology showed that the numbers of growth-hormone (GH) producing cells in the pituitary anterior lobe were severely reduced in 3 of 6 KA/KA neonates (Figure 5B). However, TUNEL-positive cells were as rare in GH-deficient mutant pituitaries as in control glands (Figure 5C), indicating that the reduction in GH-producing cells in KA/KA neonates was not due to increased apoptosis. Proliferation of mutant pituitary cells was also normal as determined by Ki-67 immunohistochemistry (data not shown). Although prolactin is known to be a mitogen and survival factor for lymphocytes in stressed animals (Dorshkind and Horseman, 2000), the number of prolactin-secreting cells in the pituitary anterior lobe was not reduced in juvenile KA/KA mice with either thymic atrophy or the spin phenotype (Figure 5D). Closer histological and immunohistochemical examination of pituitaries from P1–21 KA/KA mice with thymic atrophy or the spin phenotype revealed a relatively normal internal gland structure as well as wt expression of the transcription factor

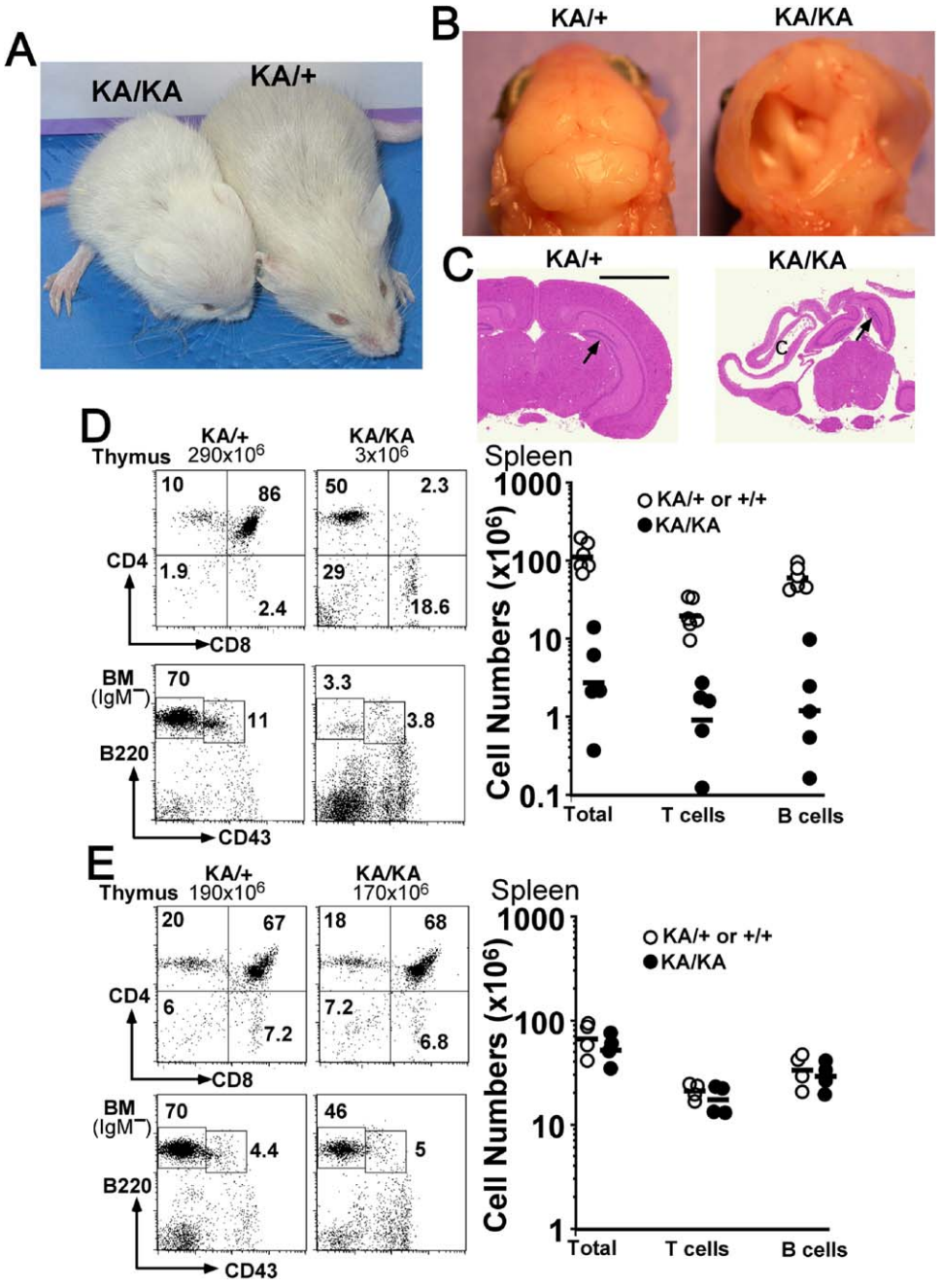

Figure 4. Cachexia, Hydrocephalus, and Extrinsic Lymphopenia in Juvenile KA/KA Mice

(A) Cachexia. Gross comparison of a KA/KA mouse with cachexia and a control KA/+ mouse at age 3.5 weeks.

(B) Hydrocephalus. Dorsal in situ views of the intact brains of KA/+ and KA/KA mice at P20 (same magnification). The mutant brain appears expanded.

(C) H&E staining of coronal sections at the level of the hippocampus through the P20 KA/+ and KA/KA brains. The fluid supporting the outer mantle layers of the mutant neocortex has drained away during processing, resulting in the collapse of the mantle (c). Arrows indicate the dentate gyrus of the hippocampus. Scale bar = 2 mm.

(D) Lymphopenia in KA/KA mice. Left panel shows flow cytometric analyses of T cell development in thymus and B cell development in the BM. Right panel shows splenic cellularity. Each circle represents an individual mouse, and horizontal bars represent geometric means.

(E) Reconstitution of lymphocyte development and cellularity. BM of KA/KA mice was transferred into *Rag-1*$^{-/-}$ mice, and the same assessments as in (D) were carried out at age 2–3 months. Left panel shows representative analyses of the 4–6 mice examined per genotype.

PIT1, thyroid-stimulating hormone, follicle-stimulating hormone, ACTH, and vasopressin (data not shown). Target organs regulated by the hypothalamic-pituitary axis (thyroid and adrenal glands and kidneys) were histologically normal. No evidence of acute tubular necrosis was seen in the kidneys of moribund mutants, indi-

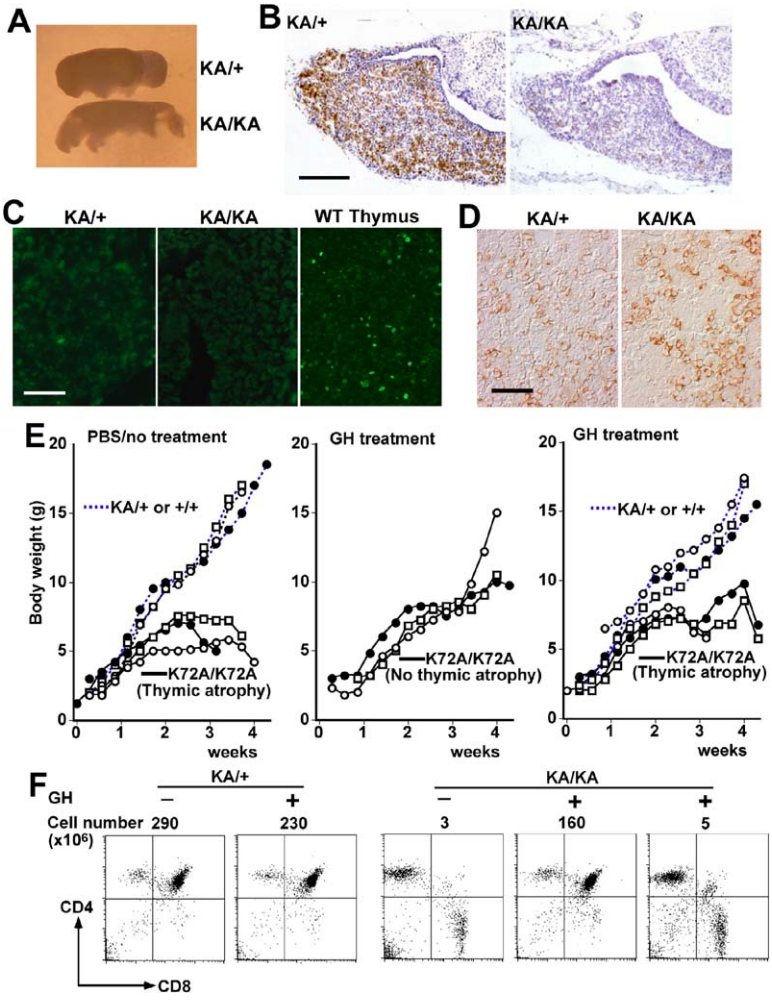

Figure 5. Partial Prevention of Lymphopenia by Growth-Hormone Administration

(A) Gross morphology of KA/+ and KA/KA pituitary glands.

(B) Immunohistochemical staining of KA/+ (left) and KA/KA (right) pituitary glands with anti-GH antibody (brown). The mutant shows a striking absence of GH. Scale bar = 150 μm.

(C) TUNEL staining of pituitary sections. Apoptotic cells (bright green dots) are equally rare in KA/+ and KA/KA pituitary tissues. A section of wt thymus was analyzed as a positive control. Scale bar = 75 μm.

(D) Immunohistochemical staining of control and KA/KA pituitary glands with anti-prolactin antibody (brown). The mutant shows normal numbers of prolactin-producing cells. Scale bar = 75 μm.

(E) Increased body weight and decreased thymic atrophy after GH treatment. Left: three untreated or PBS-treated mutants showed decreased body weight and thymic atrophy compared to controls. Middle: three mutants showed increased body weight and no thymic atrophy after GH treatment. Right: three mutants continued to show thymic atrophy and decreased body weight even after GH treatment. Each symbol represents an individual mouse.

(F) Flow cytometric analysis of thymocytes from the mice in (E). The left two panels show thymocyte numbers and CD4/CD8 expression in control mice without and with GH. The right three panels show thymocyte numbers and CD4/CD8 expression in an untreated mutant, a mutant treated with GH that responded, and a mutant treated with GH that did not respond. One experiment representative of three is shown.

cating that their rapid weight loss was not due to dehydration caused by kidney defects.

Significantly, the incidence of wasting and thymic atrophy in viable KA/KA mice correlated with the GH defect. Thymic atrophy and immunodeficiency are also present in dwarf (dw/dw) mice, which lack anterior pituitary hormones (including GH). The immune-system deficits in dw/dw mice can be reversed by GH treatment (Reichlin, 1993). To determine if a lack of GH accounted for the development of thymic atrophy in KA/KA mice, we treated neonatal pups from KA/+ × KA/+ or KA/KA × KA/+ breedings with GH every other day for 3–4 weeks. Among the GH-treated mice, six were KA/KA mutants exhibiting a wide skull and early signs of wasting. Compared to PBS-treated or -untreated mutant mice, 3 of 6 GH-treated KA/KA mice showed no loss of body weight at age 3–4 weeks (Figure 5E, left and middle panels) and had relatively normal thymi containing $CD4^+CD8^+$ cells (Figure 5F). Numbers of T and B cells in the spleens of these animals were also relatively normal (data not shown). However, the three remaining GH-treated KA/KA mice still developed thymic atrophy and severe wasting comparable to that seen in untreated or PBS-treated KA/KA mice (Figure 5E, left and right panels and Figure 5F). Thus, a lack of GH only partially accounts for the wasting and lymphopenia observed in KA/KA mice.

KA/KA mice exhibiting wasting usually became moribund at the age of 3–4 weeks, losing about 15%–20% of their body weight within 2–3 days (Figure 5E, left panel). Of the 10 moribund mice analyzed, all mice that developed hydrocephalus also displayed thymic atrophy and lymphopenia (Figures 4B–4D and data not shown). Thus, the development of lymphopenia and hydrocephalus appear linked in wasting KA/KA mice.

Lack of Cyt c-Mediated Apoptosis Leads to Development of Splenomegaly and Lymphadenopathy

Mice deficient for upstream elements of mitochondrial apoptosis (such as *Bim*$^{-/-}$ and *Bax*$^{-/-}$*Bak*$^{-/-}$ mice) display splenomegaly and lymphadenopathy due to defects in activated-T-cell death (Bouillet et al., 1999; Lindsten et al., 2000; Hildeman et al., 2002; Rathmell et al., 2002). While *Rag-1*$^{-/-}$ mice reconstituted with BM cells from moribund KA/KA mice with hydrocephalus, cachexia, and lymphopenia showed normal lymphocyte development and cellularity 2–3 months after transfer (Figure 4E), 3 of 7 reconstituted mice developed splenomegaly and lymphadenopathy 12 months

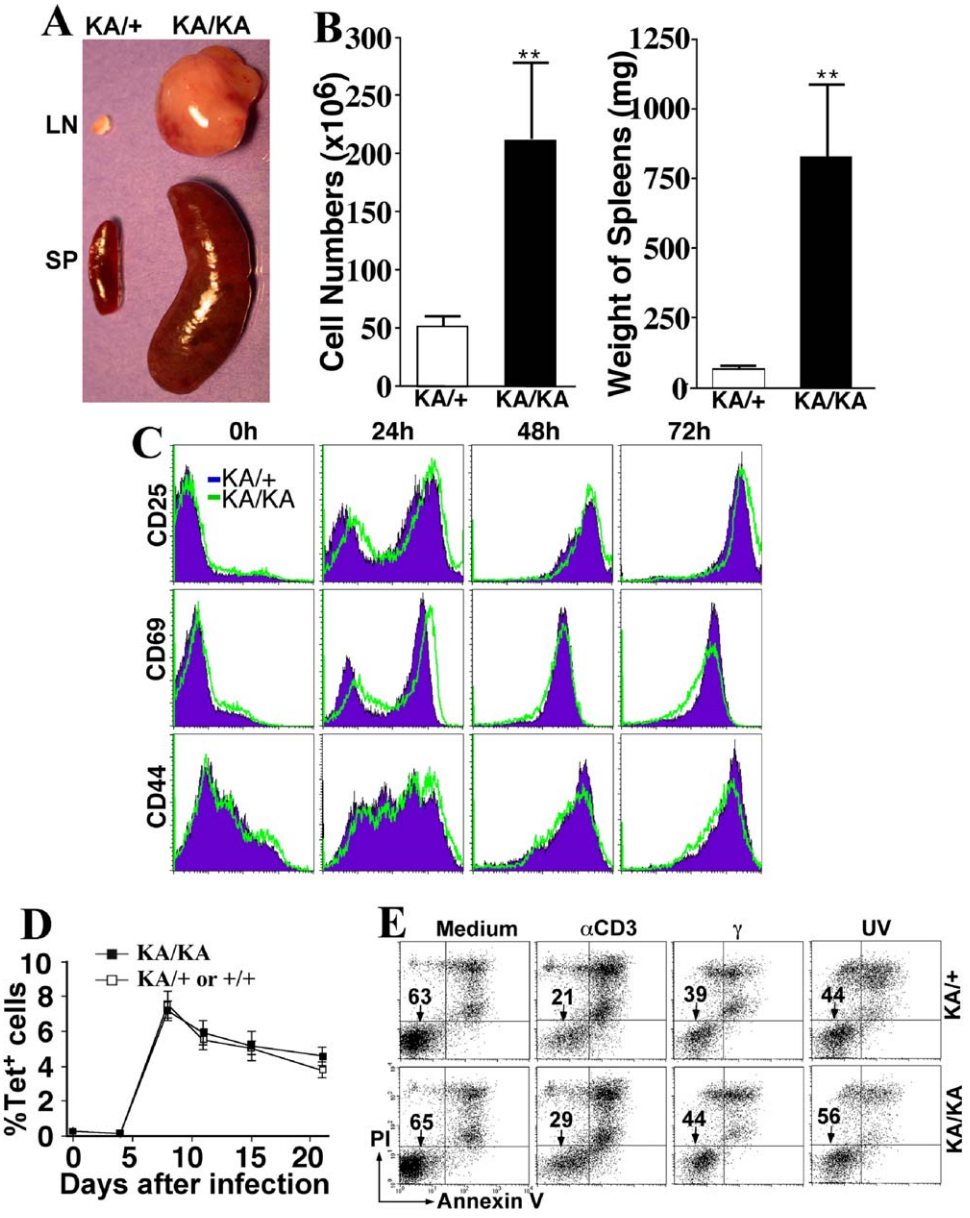

Figure 6. Splenomegaly and Lymphadenopathy in Aged Reconstituted Mice

(A) Gross morphology of lymph nodes and spleens of reconstituted *Rag-1*$^{-/-}$ mice 1 year after transfer of BM from KA/+ or wasting KA/KA mice. Seven mice per genotype were reconstituted, and 3 of 7 *Rag-1*$^{-/-}$ KA/KA mice developed the expanded phenotype shown.

(B) Mean splenic cellularities (left panel) and splenic weights (right panel) ± SD of the mice in (A). **$p < 0.05$.

(C) T cell activation kinetics. T cells from *Rag-1*$^{-/-}$ KA/KA or *Rag-1*$^{-/-}$ KA/+ mice were treated with anti-CD3 (1.0 μg/ml) plus anti-CD28 (1.0 μg/ml), and expression of the indicated activation markers was assessed by flow cytometry.

(D) Normal response to LCMV infection and clearance of GP_{33-41}-specific $CD8^+$ T cells in KA/KA mice. Mean percentages ± SEM of $CD8^+$ T cells staining positively with specific tetramer (Tet^+) are shown (n = 5).

(E) Slight resistance of activated KA/KA T cells to AICD and apoptosis in vitro. Activated T cells from KA/+ and KA/KA mice were induced to undergo AICD by CD3 religation (1.0 μg/ml) and to undergo apoptosis by exposure to γ (300 rads) or UV (40 mJ/cm^2) irradiation. Percent viability was determined 24 hr later by PI/annexin V staining and flow cytometry. Data show representative analyses of the five mice examined per genotype.

after transfer (Figure 6A). Splenic cellularity (Figure 6B, left panel) and spleen weights (Figure 6B, right panel) were increased over controls by 4-fold and 15-fold, respectively. Over 90% of the T cells present were $CD62L^{low}/CD44^{high}$ activated/memory T cells (data not shown). Likewise, the majority of B cells had an activated phenotype as judged by their larger size and upregulation of CD69 (data not shown).

We next examined the kinetics of in vitro T cell activation induced by anti-CD3 plus anti-CD28 ligation in T cells from reconstituted mice 4–6 weeks after BM or fetal liver transfer. Upregulation of the activation mark-

ers CD25, CD69, and CD44 was comparable in KA/KA and control T cells at 24 hr, 48 hr, and 72 hr (Figure 6C). In addition, KA/KA T cells proliferated normally in response to TCR-CD3 engagement (data not shown). Taken together, these results suggest that the KA/KA T cells can be activated normally to initiate an immune response.

To evaluate the effect of the KA mutation on activated-T-cell death in vivo, we infected KA/KA and littermate control mice with lymphocytic choriomeningitis virus (LCMV) and monitored changes in the proportion of LCMV $GP_{33–41}$-specific $CD8^+$ T cells in peripheral blood using PE-conjugated H-$2D^b$/$GP_{33–41}$ (KAVYNF ATM) tetramers. For both control and KA/KA mice, the proportion of cells staining positively with the tetramer declined after peaking at day 8 (Figure 6D). Thus, Cyt c-mediated apoptosis is dispensable for activated-T-cell death in the context of in vivo LCMV infection. However, activated T cells isolated from KA/KA mice with the spin phenotype were slightly resistant to in vitro activation-induced cell death (AICD) induced by CD3 religation or γ or UV irradiation (Figure 6E). Comparable results were obtained for similarly treated activated T cells from *Rag-1*$^{-/-}$ KA/KA mice (data not shown) and for naive splenocytes treated with etoposide or γ or UV irradiation (data not shown). This resistance implies an intrinsic lymphocyte defect that could contribute to chronic lymphocyte accumulation. Thus, the apoptotic function of Cyt c is both extrinsically and intrinsically involved in the maintenance of lymphocyte homeostasis.

An Apoptosome-Independent Pathway of Caspase Activation in KA/KA Thymocytes

Thymic negative selection is impaired in the absence of either *Bim* alone or *Bax* and *Bak* together (Bouillet et al., 2002; Rathmell et al., 2002). However, thymocyte development and thymic cellularity in KA/KA mice with the spin phenotype were normal (data not shown). Furthermore, thymocytes from these mutants were normally sensitive to a wide range of apoptotic stimuli, including dexamethasone, etoposide, γ irradiation, and UV irradiation (Figure 7A). In contrast, except in the case of UV, *Apaf-1*$^{-/-}$ thymocytes showed a partial resistance to all of these stimuli that was most obvious at high doses. KA/KA and *Apaf-1*$^{-/-}$ thymocytes were equally sensitive to death induced by anti-CD3 plus anti-CD28 crosslinking, Fas ligation, or neglect. To rule out the possibility that the sensitivity of KA/KA thymocytes was due to a neurological abnormality, we repeated these experiments using thymocytes from *Rag-1*$^{-/-}$ mice reconstituted with BM from wasting KA/KA, *Apaf-1*$^{-/-}$ together with control mice and confirmed that KA/KA thymocytes are sensitive to induction of apoptosis (Figure 7A).

Previous biochemical data (Wang, 2001) have suggested that Apaf-1 is the only downstream target of Cyt c. The similarities of the neuronal abnormalities in KA/KA and *Apaf-1*$^{-/-}$ mice and the resistance of KA/KA and *Apaf-1*$^{-/-}$ MEFs to apoptotic stimuli support this notion. However, the sensitivity of KA/KA thymocytes to apoptotic stimuli suggests that other Cyt c targets may exist. We performed extensive biochemical analyses to dissect apoptotic signaling in KA/KA thymocytes. Surprisingly, procaspase-9 and procaspase-3 were as efficiently cleaved in γ-irradiated KA/KA thymocytes as in controls (Figure 7B), even though Apaf-1 failed to oligomerize (Figure 7C). This result stands in contrast to UV-treated KA/KA MEFs, where impaired caspase activation (Figures 2D and 3D) was associated with an absence of Apaf-1 oligomerization (Figure 3E). Our data thus indicate that an apoptosome-independent pathway of caspase activation exists in KA/KA thymocytes. Furthermore, flow cytometric analysis showed that the kinetics of procaspase-9 and procaspase-3 cleavage in γ-irradiated KA/KA thymocytes were comparable to controls (Figure 7D). Interestingly, about 50% and 23% of γ-irradiated *Apaf-1*$^{-/-}$ thymocytes exhibited activation of caspase-9 and caspase-3, respectively, at 24 hr postirradiation. Parallel to the case of procaspase-9 cleavage, the cleavage of two other initiator caspases, procaspase-2 and procaspase-8, occurred normally in γ-irradiated KA/KA thymocytes, whereas the activation of these procaspases was delayed in γ-irradiated *Apaf-1*$^{-/-}$ cells (Figure S2, upper panel). As expected, procaspase-8 was processed similarly in KA/KA, *Apaf-1*$^{-/-}$, and control thymocytes upon activation of the death receptor Fas by anti-Fas antibody Jo-2 (Figure S2, lower panel). These observations support the hypothesis that caspases can be cleaved in an apoptosome-independent manner during stress-induced thymocyte death. Furthermore, the Apaf-1 monomer appears to be a potential positive regulator of this pathway.

To determine whether caspase activity caused the death of the KA/KA and *Apaf-1*$^{-/-}$ cells, γ-irradiated thymocytes were cultured in the presence of the pancaspase inhibitor Z-VAD-FMK. The apoptosis of both KA/KA and control thymocytes was largely inhibited in the presence of Z-VAD-FMK at 20 hr and 40 hr after γ irradiation (Figure S3A). The inhibitory effect was also observed in *Apaf-1*$^{-/-}$ thymocytes at 40 hr poststimulation (Figure S3, right). These data indicate that caspase activity operating independently of the apoptosome may be required for stress-induced death in both KA/KA and *Apaf-1*$^{-/-}$ thymocytes.

Discussion

It has been difficult to selectively assess the role of Cyt c-mediated apoptosis in development and tissue homeostasis in an intact animal because Cyt c null embryos die before the formation of most organs (Li et al., 2000). Since the embryonic lethality of Cyt c null mutants is most likely caused by a defect in oxidative phosphorylation, we devised a mouse model in which lysine 72 of Cyt c was mutated to alanine such that the mutated Cyt c protein retains normal respiratory function but lacks apoptotic function due to a failure to oligomerize Apaf-1. The KA mutation results in a neurological phenotype similar to that seen in *Apaf-1*, *caspase-9*, and *caspase-3* null mice (Cecconi et al., 1998; Hakem et al., 1998; Kuida et al., 1998; Kuida et al., 1996; Woo et al., 1998; Yoshida et al., 1998). In all of these mutants, embryonic or perinatal lethality is caused by CNS defects. The cachexia and spin phenotype seen in viable KA/KA mice also occur in one strain of *Apaf-*

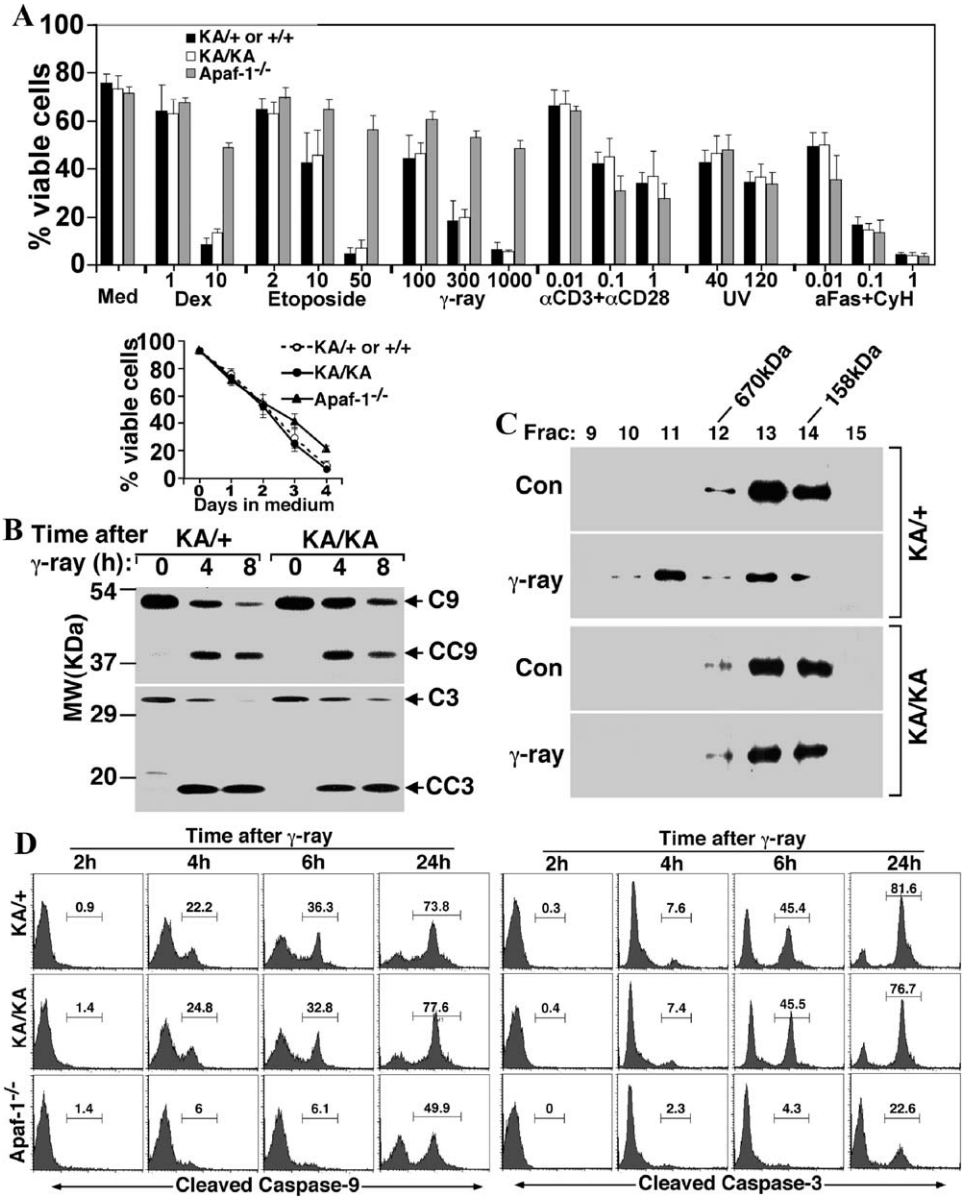

Figure 7. Normal Caspase Activation and Death of KA/KA Thymocytes in Response to Apoptotic Stimuli

(A) Upper panel: viability of thymocytes after treatment with dexamethasone (Dex; 1–10 nM), etoposide (2–50 μM), γ irradiation (300–1000 rads), anti-CD3 antibody (1.0 μg/ml) plus anti-CD28 (0.01–1.0 μg/ml), UV irradiation (40–120 mJ/cm^2), or anti-Fas antibody Jo-2 (1.0 μg/ml) plus cycloheximide (CyH, 0.01–1.0 μg/ml). Lower panel: viability kinetics of control, KA/KA, and *Apaf-1*$^{-/-}$ thymocytes cultured in RPMI containing 10% FCS (death by neglect). For both the upper and lower panels, viability was determined at 20 hr poststimulation by PI/annexin V staining followed by flow cytometry. Mean percentages of viable cells ±SD (n = 4–8) are shown. Data shown for etoposide, UV, and anti-Fas antibody are the combined analyses of thymocytes from intact KA/+, KA/KA, or *Apaf-1*$^{-/-}$ mice or from *Rag-1*$^{-/-}$ mice reconstituted with BM from control (KA/+ or +/+), KA/KA, or *Apaf-1*$^{-/-}$ mice. Data shown for the remaining apoptotic stimuli, the medium control, and the viability-kinetics panel are from the reconstituted mice only.

(B) Western blot showing normal procaspase-9 and procaspase-3 cleavage in KA/KA thymocytes subjected to γ irradiation (500 rads).

(C) Defective Apaf-1 oligomerization. Extracts of γ-irradiated (500 rads) thymocytes were fractionated according to molecular weight. Apaf-1 monomers and oligomers were located in fractions 13/14 and 10/11, respectively.

(D) Normal kinetics of procaspase-9 and procaspase-3 cleavage in KA/KA thymocytes. KA/KA, KA/+, or *Apaf-1*$^{-/-}$ thymocytes from *Rag-1*$^{-/-}$ chimeric mice were γ irradiated (500 rads), and the cleavage of procaspase-9 (left) and procaspase-3 (right) was monitored by flow cytometry over the indicated time course.

1$^{-/-}$ mice (Honarpour et al., 2000). This observation, plus the fact that KA/KA mice exhibit variable viability, suggests that genetic background greatly influences the manifestation of defects in the mitochondrial apoptotic pathway. Indeed, the incidence of cachexia and hydrocephalus among viable KA/KA mice was reduced

from 60% to <20% when the animals were backcrossed to C57BL/6 mice four to nine times (data not shown). Taken together, these observations indicate that unknown genes in the genetic background have a profound influence on the phenotype of KA/KA mice.

Although *Apaf-1*$^{-/-}$ and KA/KA mice share many similarities, there are some striking differences. First, the apparent involvement of the hypothalamic-pituitary axis and the development of lymphopenia and hydrocephalus are unique to perinatal KA/KA survivors. The distortions of the pituitary seen in some KA/KA mice are likely due to increased intracranial pressure resulting from the overexpansion of cell populations in the cortex and/or midbrain. Disruption of the hypothalamic-pituitary axis, along with aberrant cranial blood flow and CSF circulation in the brain, could impair normal homeostatic processes. The partial rescue of some KA/KA mutants with cachexia by the injection of GH suggests that the hypothalamic-pituitary axis may be disrupted in these animals. It is known that the hypothalamus controls metabolic homeostasis and is essential for successful postnatal development. For example, mice lacking the POU-domain transcription factor Brn-2 die by P10 because they fail to develop hypothalamic neurons (Nakai et al., 1995; Schonemann et al., 1995). The hypothalamus is also involved in modulating the immune response (Buller et al., 2003; Hefco et al., 2004; Wrona et al., 2003). Direct connections between the hypothalamus and brain stem are activated during an immune challenge, and mechanical destruction of these connections induces neutropenia and lymphopenia and impairs the primary immune response (Buller et al., 2003; Hefco et al., 2004). Although defects in the link between the hypothalamus, pituitary, and brain stem were not directly demonstrated in this study, we believe that the observed destruction of the neocortex, combined with pressure exerted by the hypertrophic brain on the hypothalamus, likely leads to the disruption of sufficient physiological processes to cause the death of KA/KA mutants.

The second marked difference between *Apaf-1*$^{-/-}$ and KA/KA mice arises in the susceptibility of their thymocytes to apoptosis. Both *Apaf-1*$^{-/-}$ and *caspase-9*$^{-/-}$ thymocytes are partially resistant to a variety of apoptotic stimuli (Hakem et al., 1998; Kuida et al., 1998; Yoshida et al., 1998; and Figure 7A), while thymocytes derived from lethally irradiated mice reconstituted with *Apaf-1*$^{-/-}$ and *caspase-9*$^{-/-}$ fetal liver cells show milder resistance (Marsden et al., 2002). However, KA/KA thymocytes remain sensitive to a broad range of apoptotic stimuli (Figure 7A). In contrast, KA/KA MEFs are nearly as resistant to apoptotic stimuli as *Apaf-1*$^{-/-}$ MEFs due to their impaired Apaf-1 oligomerization and caspase activation (Figure 3). While γ-irradiated KA/KA thymocytes also show an absence of Apaf-1 oligomerization, they retain the ability to efficiently activate caspases. Thus, a pathway of apoptosome-independent caspase activation exists that dominates in thymocytes but does not operate in MEFs. Interestingly, the fact that *Apaf-1*$^{-/-}$ thymocytes from *Rag-1*$^{-/-}$ chimeric mice show a low level of delayed caspase activation indicates that Apaf-1 may positively regulate this pathway.

The K72A mutation resulted in both intrinsic and extrinsic defects in lymphocyte homeostasis. The intrinsic defect was evidenced by the splenomegaly and lymphadenopathy that developed in aged *Rag-1*$^{-/-}$ KA/KA chimeric mice. Disruption of *Bim* alone or *Bax* plus *Bak* leads to a similar accumulation of memory T cells that enlarges the spleen and lymph nodes. Cyt c release is an important downstream target of Bax and Bak because *Bax*$^{-/-}$*Bak*$^{-/-}$ MEFs are completely resistant to tBID-induced Cyt c release and apoptosis (Wei et al., 2001). However, while splenomegaly and lymphadenopathy are seen at age 3–4 months in *Bax*$^{-/-}$*Bak*$^{-/-}$ mice, they are not manifested until age 12 months in *Rag-1*$^{-/-}$ KA/KA mice. Lethally irradiated mice reconstituted with fetal liver from *Apaf-1*$^{-/-}$ or *caspase-9*$^{-/-}$ mice show normal lymphocyte cellularity 10–20 weeks after transfer (Marsden et al., 2002), but it is not known whether these animals later develop enlarged spleens or lymph nodes. The delay in lymphocyte accumulation in *Rag-1*$^{-/-}$ KA/KA chimeric mice compared to *Bim*$^{-/-}$ or *Bax*$^{-/-}$*Bak*$^{-/-}$ mice supports our contention that upstream mitochondrial molecules have a target(s) other than Cyt c. Indeed, Bax- and Bak-mediated mitochondrial permeabilization causes the release of not only Cyt c but also endonuclease G (EndoG), Smac/Diablo, and Omi/HtrA2 (Danial and Korsmeyer, 2004; Jiang and Wang, 2004). One or more of these factors may act downstream of Bax and Bak to regulate lymphocyte homeostasis, although direct evidence is lacking. It is also possible that lymphocyte homeostasis can be maintained through a caspase-independent death pathway that is activated in the absence of Cyt c-mediated apoptosis. For example, in vivo Fas-mediated hepatocyte apoptosis is associated with a substantial loss of Cyt c that leads to progressive caspase-independent mitochondrial dysfunction (Mootha et al., 2001).

The extrinsic defect in lymphocyte homeostasis was evidenced by the fact that the thymic atrophy and lymphopenia phenotypes seen in KA/KA mice resolved in *Rag-1*$^{-/-}$ KA/KA chimeric mice. The reduced GH production observed in some KA/KA mice may be relevant here, although there is controversy concerning the effect of reduced GH on thymopoiesis. In dw/dw mice, which have a pituitary-gland deficiency, thymic atrophy is observed by some groups but not others (Dorshkind and Horseman, 2000). Housing conditions can have a drastic effect, as thymic cellularity is normal when dw/dw mice are housed alone but markedly reduced when they are kept with their normal-sized littermates (Dorshkind et al., 2003). In KA/KA mice, it may be that stress in the form of hydrocephalus combines with GH deficiency to trigger thymic atrophy. However, there must be additional factors involved because the lymphopenia in 50% of surviving KA/KA mice could not be prevented by GH.

In conclusion, we have taken a genetic approach to definitively demonstrate that Cyt c is essential for the apoptosis required for normal brain development and lymphocyte homeostasis in mice. Specific disruption of Cyt c's apoptotic function has also revealed the existence of an apoptosome-independent caspase activation pathway in thymocytes. Finally, we have shown that GH defects may be associated with lymphocyte loss, highlighting the substantial impact of the hypothalamic-pituitary axis on immune-system regulation.

Experimental Procedures

Please also see Supplemental Data.

Immunoblotting

Cell pellets were resuspended in 4 vol buffer A (20 mM HEPES-KOH [pH 7.5], 10 mM KCl, 1.5 mM $MgCl_2$, 1 mM Na EDTA, 1 mM Na EGTA, 1 mM DTT, and 0.1 mM PMSF), and cell extracts were prepared as described (Liu et al., 1996). Proteins were separated by SDS-PAGE and probed with antibodies against precursor or cleaved forms of caspase-3 and -9 (Cell Signaling) and *Apaf-1* (Zou et al., 1999). In vitro assays of caspase-3 and -9 activation were performed in the presence of dATP (Amersham Pharmacia Biotech) as described previously (Liu et al., 1996).

Apaf-1 Oligomerization

MEFs treated with UV (10 mJ/cm^2) or thymocytes treated with γ irradiation (500 rads) were harvested 12 hr and 4 hr later, respectively. S-100 proteins were prepared and loaded directly onto a Superdex-200 gel filtration column (Amersham Pharmacia Biotech) and eluted with buffer A. Fractions of 100 μl were collected and subjected to 8% SDS-PAGE followed by Western blotting using a rabbit antibody against Apaf-1 as described previously (Li et al., 2000).

Mitochondrial Oxygen Consumption

MEFs (1×10^6) were resuspended in 1 ml ice-cold mitochondrial isolation buffer (MIB) (200 mM mannitol, 70 mM sucrose, 10 mM HEPES [pH 7.5], and 1 mM EGTA). After 30 min on ice, the cells were disrupted by 25 passes through a 1 ml Knotes Dounce homogenizer with B pestle (Knotes Glass Company). Permeabilized cells were centrifuged at 10,000 × g for 5 min at 4°C followed by three washes in MIB. Pellets were resuspended in 200 μl MIB and stored on ice. Oxygen consumption was measured, as previously described (Mootha et al., 2001), in 600 μl stirred respiratory chambers fitted with oxygen electrodes (Instech Laboratories, Inc.). The reaction was initiated by adding 2.5×10^5 permeabilized cells to respiratory buffer (250 mM sucrose, 2 mM EGTA, 30 mM KH_2PO_4, 5 mM $MgCl_2$ and 50 mM Tris [pH 7.4]). Succinate (5 mM) and ADP (0.1 mM final concentration) were added as carbon substrates for state 4 and state 3 respiration, respectively.

Flow Cytometric Analyses

Single-cell suspensions were prepared from thymus, BM, spleen, or lymph nodes. Cells (1×10^6) were stained with fluorochrome- (FITC, PE, or Cychrome) or biotin-conjugated monoclonal antibodies followed by flow cytometry. Streptavidin-Cychrome was used to visualize biotinylated antibodies. Antibodies against CD3, CD4, CD8, CD25, CD43, CD44, CD62L, CD69, CD95, B220, IgM, and IgD were purchased from BD Bioscience. Staining of thymocytes to detect active caspase-3 (BD Biosciences) by flow cytometry was performed according to the manufacturer's instructions. Carboxyfluorescein-labeled caspase inhibitors (B-Bridge International Inc.) were used to detect cleaved caspase-2, -8, and -9 according to the manufacturer's instructions.

Supplemental Data

Supplemental Data include Supplemental Experimental Procedures, three figures, two tables, and Supplemental References and are available with this article online at http://www.cell.com/cgi/content/full/121/4/579/DC1/.

Acknowledgments

We thank M. Capecchi for the ACN cassette, S. Asa for advice on the endocrine-gland work, G. Oleg and K. Tatsuya for help with the O_2 consumption measurements, N.J. Chen for help with the graphics, A.F. Parlow for the GH and related antibodies, various Mak lab members for helpful discussions, and M. Saunders for scientific editing. This work was supported by the Terry Fox Cancer Foundation and National Cancer Institute of Canada (T.W.M.) and NIH grant GMRO1-57158 (M.F. and X.W.).

Received: October 8, 2004
Revised: January 12, 2005
Accepted: March 14, 2005
Published: May 19, 2005

References

Bouillet, P., Metcalf, D., Huang, D.C., Tarlinton, D.M., Kay, T.W., Kontgen, F., Adams, J.M., and Strasser, A. (1999). Proapoptotic Bcl-2 relative Bim required for certain apoptotic responses, leukocyte homeostasis, and to preclude autoimmunity. Science *286*, 1735–1738.

Bouillet, P., Purton, J.F., Godfrey, D.I., Zhang, L.C., Coultas, L., Puthalakath, H., Pellegrini, M., Cory, S., Adams, J.M., and Strasser, A. (2002). BH3-only Bcl-2 family member *Bim* is required for apoptosis of autoreactive thymocytes. Nature *415*, 922–926.

Buller, K.M., Dayas, C.V., and Day, T.A. (2003). Descending pathways from the paraventricular nucleus contribute to the recruitment of brainstem nuclei following a systemic immune challenge. Neuroscience *118*, 189–203.

Cecconi, F., Alvarez-Bolado, G., Meyer, B.I., Roth, K.A., and Gruss, P. (1998). Apaf1 (CED-4 homolog) regulates programmed cell death in mammalian development. Cell *94*, 727–737.

Chao, D.T., Linette, G.P., Boise, L.H., White, L.S., Thompson, C.B., and Korsmeyer, S.J. (1995). Bcl-XL and Bcl-2 repress a common pathway of cell death. J. Exp. Med. *182*, 821–828.

Danial, N.N., and Korsmeyer, S.J. (2004). Cell death: critical control points. Cell *116*, 205–219.

Dorshkind, K., and Horseman, N.D. (2000). The roles of prolactin, growth hormone, insulin-like growth factor-I, and thyroid hormones in lymphocyte development and function: insights from genetic models of hormone and hormone receptor deficiency. Endocr. Rev. *21*, 292–312.

Dorshkind, K., Welniak, L., Gault, R.A., Hixon, J., Montecino-Rodriguez, E., Horseman, N.D., Gertner, J.M., and Murphy, W.J. (2003). Effects of housing on the thymic deficiency in dwarf mice and its reversal by growth hormone administration. Clin. Immunol. *109*, 197–202.

Green, D.R., and Reed, J.C. (1998). Mitochondria and apoptosis. Science *281*, 1309–1312.

Grillot, D.A., Merino, R., and Nunez, G. (1995). Bcl-XL displays restricted distribution during T cell development and inhibits multiple forms of apoptosis but not clonal deletion in transgenic mice. J. Exp. Med. *182*, 1973–1983.

Hakem, R., Hakem, A., Duncan, G.S., Henderson, J.T., Woo, M., Soengas, M.S., Elia, A., de la Pompa, J.L., Kagi, D., Khoo, W., et al. (1998). Differential requirement for caspase 9 in apoptotic pathways in vivo. Cell *94*, 339–352.

Hefco, V., Olariu, A., Hefco, A., and Nabeshima, T. (2004). The modulator role of the hypothalamic paraventricular nucleus on immune responsiveness. Brain Behav. Immun. *18*, 158–165.

Hengartner, M.O. (2000). The biochemistry of apoptosis. Nature *407*, 770–776.

Hildeman, D.A., Zhu, Y., Mitchell, T.C., Bouillet, P., Strasser, A., Kappler, J., and Marrack, P. (2002). Activated T cell death in vivo mediated by proapoptotic bcl-2 family member Bim. Immunity *16*, 759–767.

Honarpour, N., Du, C., Richardson, J.A., Hammer, R.E., Wang, X., and Herz, J. (2000). Adult Apaf-1-deficient mice exhibit male infertility. Dev. Biol. *218*, 248–258.

Jiang, X., and Wang, X. (2004). Cytochrome C-mediated apoptosis. Annu. Rev. Biochem. *73*, 87–106.

Kluck, R.M., Esposti, M.D., Perkins, G., Renken, C., Kuwana, T., Bossy-Wetzel, E., Goldberg, M., Allen, T., Barber, M.J., Green, D.R., and Newmeyer, D.D. (1999). The pro-apoptotic proteins, Bid and Bax, cause a limited permeabilization of the mitochondrial outer membrane that is enhanced by cytosol. J. Cell Biol. *147*, 809–822.

Kluck, R.M., Ellerby, L.M., Ellerby, H.M., Naiem, S., Yaffe, M.P., Margoliash, E., Bredesen, D., Mauk, A.G., Sherman, F., and Newmeyer,

D.D. (2000). Determinants of cytochrome c pro-apoptotic activity. The role of lysine 72 trimethylation. J. Biol. Chem. *275*, 16127–16133.

Kuida, K., Zheng, T.S., Na, S., Kuan, C., Yang, D., Karasuyama, H., Rakic, P., and Flavell, R.A. (1996). Decreased apoptosis in the brain and premature lethality in CPP32-deficient mice. Nature *384*, 368–372.

Kuida, K., Haydar, T.F., Kuan, C.Y., Gu, Y., Taya, C., Karasuyama, H., Su, M.S., Rakic, P., and Flavell, R.A. (1998). Reduced apoptosis and cytochrome c-mediated caspase activation in mice lacking caspase *9*. Cell *94*, 325–337.

Li, K., Li, Y., Shelton, J.M., Richardson, J.A., Spencer, E., Chen, Z.J., Wang, X., and Williams, R.S. (2000). Cytochrome c deficiency causes embryonic lethality and attenuates stress-induced apoptosis. Cell *101*, 389–399.

Li, P., Nijhawan, D., Budihardjo, I., Srinivasula, S.M., Ahmad, M., Alnemri, E.S., and Wang, X. (1997). Cytochrome c and dATP-dependent formation of Apaf-1/caspase-9 complex initiates an apoptotic protease cascade. Cell *91*, 479–489.

Lindsten, T., Ross, A.J., King, A., Zong, W.X., Rathmell, J.C., Shiels, H.A., Ulrich, E., Waymire, K.G., Mahar, P., Frauwirth, K., et al. (2000). The combined functions of proapoptotic Bcl-2 family members Bak and Bax are essential for normal development of multiple tissues. Mol. Cell *6*, 1389–1399.

Liu, X., Kim, C.N., Yang, J., Jemmerson, R., and Wang, X. (1996). Induction of apoptotic program in cell-free extracts: requirement for dATP and cytochrome c. Cell *86*, 147–157.

Ma, A., Pena, J.C., Chang, B., Margosian, E., Davidson, L., Alt, F.W., and Thompson, C.B. (1995). Bclx regulates the survival of double-positive thymocytes. Proc. Natl. Acad. Sci. USA *92*, 4763–4767.

Marsden, V.S., O'Connor, L., O'Reilly, L.A., Silke, J., Metcalf, D., Ekert, P.G., Huang, D.C., Cecconi, F., Kuida, K., Tomaselli, K.J., et al. (2002). Apoptosis initiated by Bcl-2-regulated caspase activation independently of the cytochrome c/Apaf-1/caspase-9 apoptosome. Nature *419*, 634–637.

Meier, P., Finch, A., and Evan, G. (2000). Apoptosis in development. Nature *407*, 796–801.

Mootha, V.K., Wei, M.C., Buttle, K.F., Scorrano, L., Panoutsakopoulou, V., Mannella, C.A., and Korsmeyer, S.J. (2001). A reversible component of mitochondrial respiratory dysfunction in apoptosis can be rescued by exogenous cytochrome c. EMBO J. *20*, 661–671.

Motoyama, N., Wang, F., Roth, K.A., Sawa, H., Nakayama, K., Nakayama, K., Negishi, I., Senju, S., Zhang, Q., Fujii, S., et al. (1995). Massive cell death of immature hematopoietic cells and neurons in Bcl-x-deficient mice. Science *267*, 1506–1510.

Nakai, S., Kawano, H., Yudate, T., Nishi, M., Kuno, J., Nagata, A., Jishage, K., Hamada, H., Fujii, H., Kawamura, K., et al. (1995). The POU domain transcription factor Brn-2 is required for the determination of specific neuronal lineages in the hypothalamus of the mouse. Genes Dev. *9*, 3109–3121.

Opferman, J.T., Letai, A., Beard, C., Sorcinelli, M.D., Ong, C.C., and Korsmeyer, S.J. (2003). Development and maintenance of B and T lymphocytes requires antiapoptotic MCL-1. Nature *426*, 671–676.

Rathmell, J.C., and Thompson, C.B. (2002). Pathways of apoptosis in lymphocyte development, homeostasis, and disease. Cell *109* (Suppl.), S97–S107.

Rathmell, J.C., Lindsten, T., Zong, W.X., Cinalli, R.M., and Thompson, C.B. (2002). Deficiency in Bak and Bax perturbs thymic selection and lymphoid homeostasis. Nat. Immunol. *3*, 932–939.

Reichlin, S. (1993). Neuroendocrine-immune interactions. N. Engl. J. Med. *329*, 1246–1253.

Rodriguez, J., and Lazebnik, Y. (1999). Caspase-9 and APAF-1 form an active holoenzyme. Genes Dev. *13*, 3179–3184.

Schonemann, M.D., Ryan, A.K., McEvilly, R.J., O'Connell, S.M., Arias, C.A., Kalla, K.A., Li, P., Sawchenko, P.E., and Rosenfeld, M.G. (1995). Development and survival of the endocrine hypothalamus and posterior pituitary gland requires the neuronal POU domain factor Brn-2. Genes Dev. *9*, 3122–3135.

Veis, D.J., Sorenson, C.M., Shutter, J.R., and Korsmeyer, S.J. (1993). Bcl-2-deficient mice demonstrate fulminant lymphoid apoptosis, polycystic kidneys, and hypopigmented hair. Cell *75*, 229–240.

Wang, X. (2001). The expanding role of mitochondria in apoptosis. Genes Dev. *15*, 2922–2933.

Wei, M.C., Zong, W.X., Cheng, E.H., Lindsten, T., Panoutsakopoulou, V., Ross, A.J., Roth, K.A., MacGregor, G.R., Thompson, C.B., and Korsmeyer, S.J. (2001). Proapoptotic BAX and BAK: a requisite gateway to mitochondrial dysfunction and death. Science *292*, 727–730.

Woo, M., Hakem, R., Soengas, M.S., Duncan, G.S., Shahinian, A., Kagi, D., Hakem, A., McCurrach, M., Khoo, W., Kaufman, S.A., et al. (1998). Essential contribution of caspase 3/CPP32 to apoptosis and its associated nuclear changes. Genes Dev. *12*, 806–819.

Wrona, D., Jurkowski, M., Luszawska, D., Tokarski, J., and Trojniar, W. (2003). The effects of lateral hypothalamic lesions on peripheral blood natural killer cell cytotoxicity in rats hyper- and hyporesponsive to novelty. Brain Behav. Immun. *17*, 453–461.

Wyllie, A.H. (1980). Glucocorticoid-induced thymocyte apoptosis is associated with endogenous endonuclease activation. Nature *284*, 555–556.

Yoshida, H., Kong, Y.Y., Yoshida, R., Elia, A.J., Hakem, A., Hakem, R., Penninger, J.M., and Mak, T.W. (1998). Apaf1 is required for mitochondrial pathways of apoptosis and brain development. Cell *94*, 739–750.

Yu, T., Wang, X., Purring-Koch, C., Wei, Y., and McLendon, G.L. (2001). A mutational epitope for cytochrome C binding to the apoptosis protease activation factor-1. J. Biol. Chem. *276*, 13034–13038.

Yuan, J., and Yankner, B.A. (2000). Apoptosis in the nervous system. Nature *407*, 802–809.

Zou, H., Li, Y., Liu, X., and Wang, X. (1999). An APAF-1.cytochrome c multimeric complex is a functional apoptosome that activates procaspase-9. J. Biol. Chem. *274*, 11549–11556.